



Chemical reaction and non-Darcian effects on MHD generalized Newtonian nanofluid motion

Mohamed Y. Abou-zeid

Department of Mathematics, Faculty of Education, Ain Shams University, Heliopolis, Roxy, 11757, Cairo, Egypt.



CrossMark

Abstract

The aim of this paper is to study generalized Newtonian (Carreau) nanofluid flow with heat transfer through a non-Darcy porous medium in the presence of electromagnetic field and Biot number effects. Moreover, the heat source, viscous and Ohmic dissipation, and chemical reaction effects are taken into consideration. The system of non-linear equations which govern the motion is transformed into ordinary differential equations by using a suitable similarity transformation. These equations are solved by making use of the Runge-Kutta-Merson method in a shooting and matching technique. The numerical solutions of the velocity, temperature and nanoparticles concentration are obtained as functions of the physical parameters of the problem. Moreover, the effects of these parameters on these solutions are discussed numerically and depicted graphically. It is found that both tangential and normal velocities increase or decrease as the Darcy number increases. Moreover, the temperature increases as both the Forchheimer and Reynolds numbers increase, and both the Weissenberg and Biot numbers lead to increase the nanoparticles concentration.

Keywords: Non-Newtonian nanofluid; heat transfer; non-Darcy porous medium; chemical reaction.

1. Introduction

A liquid with very small particles of diameter less than 100 nm is called nanofluid. By adding these nanoparticles up to the fluid makes it non-homogeneous, consequently, thermodynamic is in the flow increases that will cause more energy and power losses into the system. Saving helpful energy will depend on how to design the effective heat transfer process from a thermodynamic point of view. Energy transformation processes will tend to a proportional increase in entropy. Consequently, even if the energy is preserved, the high quality of energy that decreases converting them into a different form of energy at which less work can be obtained. One of the first people who added the entropy generation to the fluid flow was Bejan [1, 2]. Also, he presented a method which is called the entropy generation minimization (EGM) to measure and optimization disorder or disorganization generated during a process. There is no question that by "optimize" we mean the stable process in which the system loses the least

energy while still performing its fundamental engineering function. The method is also known as second law analysis and thermodynamic optimization. This field has been developed astoundingly during the 1990s, in both engineering and physics. Good examples of such efforts found in references [3-6].

Magnetohydrodynamics (MHD) is interested with Newtonian or non-Newtonian fluids motion and with the interaction of electrically conducting fluids. The concept of MHD was investigated by Alfvén [7]. The MHD fluid flow has received remarkable attention by scientists and researchers due to its enormous applications in the field of geophysics, mechanical, electrical, biological, geothermal as well as many other technical and industrial processes like cooling of generators, nuclear reactors, power generators, ...etc. Radially varying magnetic field effects on the Jeffery fluid peristaltic flow with heat and mass transfer in the presence of radiation and heat source was analyzed by Eldabe and Abouzeid [8]. Sheikholeslami et al. [9] studied the flow of a

*Corresponding author e-mail: master_math2003@yahoo.com; (Mohamed Y. Abou-zeid).

Receive Date: 10 April 2022, Revise Date: 21 April 2022, Accept Date: 21 April 2022

DOI: 10.21608/EJCHEM.2022.132580.5857

©2022 National Information and Documentation Center (NIDOC)

nanofluid in the presence of thermal radiation and magnetic field. MHD non-Newtonian nanofluid flow through a porous medium with couple stresses effects is discussed by Abouzeid [10]. El-dabe et al. [11] have investigated the electromagnetic steady motion of Casson fluid with heat and mass transfer through porous medium past a shrinking plate. MHD fluid flow has received remarkable attention by scientists and researchers [12-19].

Th problems in which the flow initiates from zero velocity at the wall to extreme velocity within the main flow is called boundary layer problem. The concept of boundary layer has a sence in all of viscous fluid dynamics within the hypothesis of heat transfer. The boundary layer flow with heat transfer over a stretching or shrinking plate has a great importance due to its applications including glass-fiber production, plastic pieces aero-dynamic extrusion, hot rolling and paper production. Carreau nanofluid flow over a stretching porous plate with thermal diffusion and diffusion thermo effects was studied by Eldabe et al. [20]. Kamran and Wiwatanapataphee [21] reported that chemical reaction with the Newtonian heating impact is significant in the solidification process of liquid crystals and polymeric suspensions. The boundary layer flow with heat and mass transfer properties are achieved analytically in the presence of viscous dissipation and heat source by Abouzeid [22]. Many researchers considered various non-Newtonian fluid models in their studies [23-26].

The main aim of this work is to extend the work of Eldabe et al. [11] to include Carreau nanofluid, pressure driven flow, non-Darcian porosity and Biot number effects. Then the boundary layer motion of Carreau nanofluid conducting fluid with heat transfer over a shrinking plate is analyzed. The system is stressed by both uniform magnetic and electric fields. A heat generation with radiation and chemical reaction are taken in consideration. This motion is modulated mathematically by a system of non-linear partial differential equations which transformed into non-linear ordinary differential equations by using suitable transformation. This system is solved numerically subjected to the appropriate boundary conditions in the presence of Biot number to obtain the velocity, temperature and nanoparticles concentration distributions. The influences of the physical parameters of the problem on these solutions are discussed numerically and illustrated graphically

through a set of figures. Physically, our model corresponds to the airfoils flow with low or high Reynolds number.

2 Mathematical formulations

Cartesian coordinates (x, y, z) are considered, where x is along the direction of fluid flow, y is normal to x , and z is normal to the plane (xy) . An electrically conducting Carreau nanofluid flows steadily over a shrinking sheet. The external applied magnetic field $B = (0, B_0, 0)$, while the electric field $E = (0, 0, -E_0)$.

The constitutive equation of Carreau fluid can be written as follows:

$$\tau_{ij} = -\eta_0 \left[1 + \frac{(n-1)}{2} \Gamma^2 \dot{\gamma}^2 \right] \dot{\gamma}_{ij}, \quad (1)$$

$$\dot{\gamma}_{11} = 2 \frac{\partial u}{\partial x}, \quad \dot{\gamma}_{12} = \dot{\gamma}_{21} = \frac{\partial u}{\partial y} + \frac{\partial v}{\partial x}, \quad \dot{\gamma}_{22} = 2 \frac{\partial v}{\partial y}, \quad (2)$$

where $\dot{\gamma}$ is defined as:

$$\dot{\gamma} = \sqrt{\frac{1}{2} \sum_i \sum_j \dot{\gamma}_{ij} \dot{\gamma}_{ij}} = \sqrt{\frac{1}{2} \Pi_{\dot{\gamma}}}, \quad (3)$$

where $\Pi_{\dot{\gamma}}$ is second invariant of strain-rate tensor $\dot{\gamma}_{ij}$.

The governing equations of continuity, momentum, energy, and nanoparticles concentration can be written, respectively, as

$$\frac{\partial u}{\partial x} + \frac{\partial v}{\partial y} = 0 \quad (4)$$

$$u \frac{\partial u}{\partial x} + v \frac{\partial u}{\partial y} = \frac{-1}{\rho} \frac{\partial p}{\partial x} - \frac{\eta_0}{\rho} \frac{\partial}{\partial y} \left\{ \left(1 + \frac{n-1}{2} \Gamma^2 \left(\frac{\partial u}{\partial y} \right)^2 \right) \frac{\partial u}{\partial y} \right\}, \quad (5)$$

$$\begin{aligned} & + \frac{\sigma}{\rho} (E_0 B_0 - B_0^2 u) - \frac{\nu}{k} u + C^* u^2 \\ u \frac{\partial T}{\partial x} + v \frac{\partial T}{\partial y} & = \frac{K}{\rho c_p} \frac{\partial^2 T}{\partial y^2} \\ & - \frac{\eta_0}{\rho c_p} \left\{ \left(1 + \frac{n-1}{2} \Gamma^2 \left(\frac{\partial u}{\partial y} \right)^2 \right) \frac{\partial u}{\partial y} \right\} \frac{\partial u}{\partial y} \\ & + \frac{\sigma}{\rho c_p} (u B_0 - E_0)^2 - \frac{1}{\rho c_p} \frac{\partial q_r}{\partial y} + \frac{Q_0}{\rho c_p} (T - T_\infty) \\ & + D_r \left(\frac{\partial T}{\partial y} \right)^2 + D_b \left(\frac{\partial T}{\partial y} \right) \left(\frac{\partial C}{\partial y} \right) \end{aligned} \quad (6)$$

$$u \frac{\partial C}{\partial x} + v \frac{\partial C}{\partial y} = D_B \frac{\partial^2 C}{\partial y^2} + \frac{D_T}{T_0} \frac{\partial^2 T}{\partial y^2} - A(C - C_\infty) \quad (7)$$

where the thermal radiation heat flux;

$$q_r = -\frac{4\sigma^*}{3k_0} \frac{\partial T^4}{\partial y}. \text{ We assume that the differences of}$$

fluid-phase temperature in the flow are sufficient small such that T^4 may be expressed as a linear function of temperature

Nomenclature

$$T^4 = 4T_\infty^3 T - 3T_\infty^4 \quad (8)$$

In order to simplify the above system, we use the following transformations,

$$u = -bx f'(\eta), \quad v = \sqrt{bv} f(\eta), \quad \theta = \frac{T - T_\infty}{T_0 - T_\infty}, \quad (9)$$

$$\varphi = \frac{C - C_\infty}{C_0 - C_\infty}, \quad \eta = \sqrt{\frac{b}{\nu}} y$$

A	Reaction rate constant	Pr	Prandtl number
B_0	Constant	q_r	Thermal radiation heat flux
Bi	Biot number	Q_0	Heat source parameter
C	The nanoparticles concentration	R	Radiation parameter
C^*	Forchheimer δ constant	Re	Reynolds number
c_p	The specific heat at constant pressure	Sc	Schmidt number
Da	Darcy number	T	The fluid temperature
D_B	Brownian diffusion coefficient	u	Tangential component of velocity
D_T	Thermophoretic diffusion coefficient	v	Normal component of velocity
E_0	Constant	We	Weissenberg number
E_1	Local electric parameter	x	Tangential coordinate
Ec	Eckert number	y	Normal coordinate
Fs	Forchheimer number		Greek symbols
K	Thermal conductivity	δ	Chemical reaction parameter
k	Permeability constant	η_0	Zero-shear-rate viscosity
k_0	the mean absorption coefficient	Γ	time constant
M	Magnetic field parameter	ν	Kinematic viscosity
n	dimensionless power-law index	ρ	Fluid density
N_b	Brownian motion parameter	σ	The electrical conductivity of the fluid
N_t	Thermophoresis parameter	σ^*	Stefan-Boltzmann constant
p	The fluid pressure	τ_{ij}	the stress tensor components,

Eq. (4) is automatically satisfied. Substitution of Eqs.(9) in Eqs.(5-7), we get

$$f'^2 - ff'' = -\frac{\partial p}{\partial x} - \frac{1}{Re} \left(1 + \frac{n-1}{2} We f'^{n2}\right) f'''' \quad (10)$$

$$-(M^2 - \frac{1}{Da}) f' + M^2 E_1 + Fs f'^2,$$

$$f\theta' = \frac{1+4R}{3Pr} \theta'' - \frac{Ec}{Re} \left(1 + \frac{n-1}{2} We^2 f'^{n2}\right) f'^{n2} + Ec M^2 (f' + E_1)^2 + Q_0 \theta + Nt \theta' + Nb \theta' \varphi', \quad (11)$$

$$Sc f \varphi' = \varphi'' + \frac{Nt}{Nb} \theta'' - \delta \varphi'' \quad (12)$$

It may be pointed out here that $n=1$ leads to the boundary-layer flow of ordinary Newtonian conducting fluid. While if we put $F_s = \frac{\partial p}{\partial x} = 0$, $n=1$ and

$Bi \rightarrow \infty$, this problem have been studied for the same boundary conditions by Eldabe et al. [11].Eq.(10-12) are coupled non-linear ordinary differential equation of order three. For Carreau fluid, as the parameter n tends to zero, the fluid becomes ordinary Newtonian.

The boundary conditions in the non-dimensional form are:

$$f(0) = 0, \quad f'(0) = 1, \quad \theta(0) = 1 + \frac{1}{Bi} \theta'(0), \quad (13)$$

$$\varphi(0) = 1, \quad f'(\infty) = \theta(\infty) = \varphi(\infty) = 0$$

3.Numerical solutions

NAG Fortran library with the help of subroutine D02HAF is used to solve the above system of equations (10-12). Moreover, then, shooting technique is applied. This subroutine requires to guess missing initial and terminal conditions. The governing equations (10-12) are solved by Rung-Kutta-Merson

method of order five. In this subroutine, we used variable step size in order to control the local truncation error, then, a modified Newton-Raphson method is used to obtain successive corrections for the estimated boundary values. The process is repeated iteratively many times until convergence and accuracy are occurred.

4. Discussion

In this section, both the tangential and normal velocities, temperature and nano-particles concentration for different values of the problem physical parameters are analyzed in details and depicted graphically. Mathematica package Ver.10.1

is used to obtain the numerical values of these physical quantities. The coefficients of skin-friction and both heat transfer and mass transfer are tabulated to obtain the effect of the above parameters in details. The following values of pertinent parameters are taken as follows

$$n = 2, M = 0.5, Da = 1, E1 = 1, \frac{\partial p}{\partial x} = -10, Re = 0.5, Fs = 0.4, We = 0.5, Pr = 1, R = 1, Ec = 3.5, Q0 = 1, Sc = 2.5, Bi = 0.5, Nt = 1.5, Nb = 2.5, m = 2, \delta = 0.8.$$

Pr	M	Bi	$-\theta'(0)$ in the present work	$-\theta'(0)$ in the work of Eldabe et al. [11]
1	1	0.5	1.20705	1.19268
2	1	0.5	1.89802	1.94141
3	1	0.5	2.80445	2.79731
3	0.6	0.5	1.29605	1.34502
3	0.8	0.5	1.31918	1.33632
3	1	0.5	1.24717	1.25013
3	1	0.2	0.87026	
3	1	0.1	0.76004	

Table (1)

Weissenberg number yields from the ratio between the elastic forces to the viscous forces. Moreover, it usually measures the relation of stress relaxation time of the fluid and a specific process time, i.e. Weissenberg number may help to increase the fluid motion. Figures (1) and (2) display the variations of the normal velocity f versus the dimensionless coordinate η for different values of Weissenberg number We and the magnetic field parameter M , respectively. It is noted from these figures that the normal velocity increases with the increase of We ; this is due to the above definition of Weissenberg number, while it decreases as M increases. In addition, f increases with η for large values of We , and small values of M , till a definite value $\eta = \eta_0$ (represents the maximum value of f) and it decreases afterwards. This maximum value of f increases by increasing We , while it decreases by increasing M . The result in figure (2) is due to the fact that the effect of the magnetic field on electrically conductive fluid generates a drag force and develops the force which is known as Lorentz force, and it makes to decrease the motion of fluid. Fig. (3) shows the variation of the normal velocity f with η for various values of Darcy number Da . It is seen from Fig. (3), that the normal velocity decreases with the increasing of Da in the interval $\eta \in [0, 0.85]$; otherwise, it increases by increasing Da . Therefore,

the behavior of f in the interval $\eta \in [0, 0.85]$ is opposite to its behavior in the interval $\eta \in [0.85, 1.2]$.

The variations of the tangential velocity f' with the dimensionless coordinate η for various values of the dimensionless power-law index n and Reynolds number Re are shown in Figs. (4) and (5), respectively. The graphical results of Figs. (4) and (5), indicate that the tangential velocity increases with increasing in the parameter n , while it decreases by increasing the parameter Re , respectively. Furthermore, It is observed that for small values of n and large values of Re , the relation between f' and η is a parabola with down vertex, i.e. f' decreases with η till a definite value $\eta = \eta_0$, (represents the minimum value of f') and it increases afterwards. This absolute minimum value of f' increases by increasing Re , while it decreases by increasing n . The following explains the result in Fig. (5); Reynolds number is defined as the rate of inertia forces to viscous forces in a fluid, this will lead to a resistance in fluid flow as Reynolds number increases. Moreover, this result is in agreement with those which are presented by [27].

Figs. (6) and (7) show the behavior of the temperature distribution θ with the dimensionless coordinate η for various values of the thermophoresis parameter Nt and Brownian motion parameter Nb , respectively. It has been seen from these figures that

the temperature increases with the increases of Nt , while it decreases as Nb increases. It is also noted that for each value of both Nt and Nb , there exists a minimum value of θ which its absolute value increases by increasing Nb and decreases by increasing Nt , and all minimum values occur at $\eta = 0.25$. Brownian motion is an inherent flow of particles dangled in a fluid. This random transition agrees with the fact that the temperature decreases with Brownian motion parameter. So, the result in Fig. (7) agrees with the physical expectation, and is in agreement with those which are presented by [28, 29]. The effect of Ec on the temperature distribution θ as a function of the dimensionless coordinate η is shown in Fig. (8). It is found that the temperature distribution increases by increasing Ec in the interval $\eta \in [0.5, 1.2]$; otherwise it decreases by increasing Ec . Fig. (9) illustrates the effect of Bi on the temperature distribution θ as a function of the dimensionless coordinate η . It is found that in the interval of the coordinate $\eta \in [0.18, 1.2]$, the behavior of θ for various values of Bi is exactly similar to the behavior of θ for various values of Nb given in Fig. (7). It is also noted, from Fig. (9) that in the interval of the radial coordinate $\eta \in [0, 0.18]$, except that the curves are quite close to each other in the second interval. Eq. (13) evaluates how the nanoparticles concentration distribution ϕ changes with the dimensionless coordinate η . The effects of both Biot number Bi and the local electric parameter E_1 on the nanoparticles concentration distribution ϕ are given in figures (10) and (11), respectively. It is found that the nanoparticles concentration increases by increasing Bi , but it decreases by increasing E_1 . Furthermore, the nanoparticles concentration is always positive and for large values of Bi and small values of E_1 , it increases with η till a maximum value of η , after which it decreases. The effects of Brownian motion parameter Nb on the nanoparticles concentration ϕ which is a function of η are given in Fig. (12). It is found that the nanoparticles concentration decreases by increasing Nb in the interval $\eta \in [0, 0.55]$; otherwise it increases by increasing η . So, the behavior of g in the interval $\eta \in [0, 0.55]$, is an inversed manner of its behavior in the interval $\eta \in [0.55, 1.2]$, and in the first interval, there is a maximum value of ϕ holds at $\eta = 0.19$. Figure (13) illustrates the effect of the pressure gradient $\frac{\partial p}{\partial x}$ on the nanoparticles concentration ϕ as a function of η . It is found that, the behavior of ϕ for

various values of $\frac{\partial p}{\partial x}$ is an inversed manner to the behavior of g for various values of Nb given in Figure (12). It is also noted from Fig. (13) that the nanoparticles concentration is always positive. Moreover, the relation between ϕ and η is a parabolic, i.e. as η increases, ϕ increases till a maximum value after which it decreases.

Table (1) presents a comparison between the numerical results of present study and those obtained by Eldabe et al. [18] for skin friction $f''(0)$, Nusselt number $-\theta'(0)$ and Sherwood number $-\phi'(0)$ for various values of both E_1 and Ha . It is clear from table (1) that an increase in the local electric parameter E_1 gives an increase in the skin-friction, but both Nusselt number and Sherwood number decreases or increases. Moreover, as Hartman number Ha increases, the values of $f''(0)$ and Sh increase but decreases the dimensionless quantity Nu . Finally, It can be concluded from table (1) that the present results are in a good agreement with those obtained by Eldabe et al. [19]

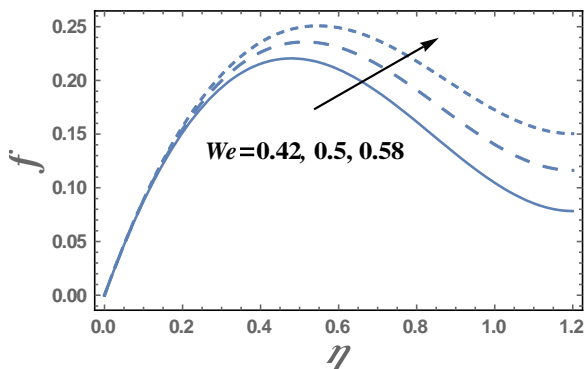


Figure 1: The normal velocity f is sketched towards η under the impact of We

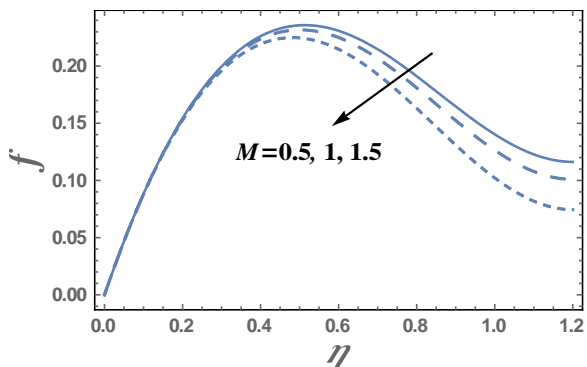


Figure 2: The normal velocity f is sketched towards η under the impact of M

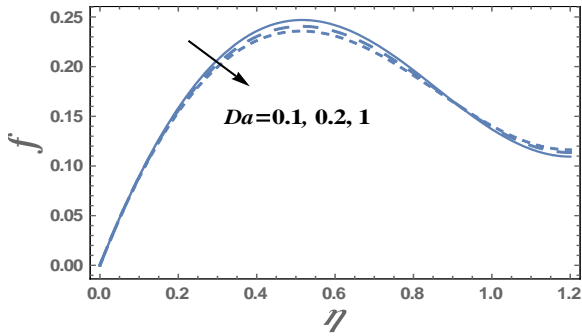


Figure 3: The normal velocity f is sketched towards η under the impact of Da

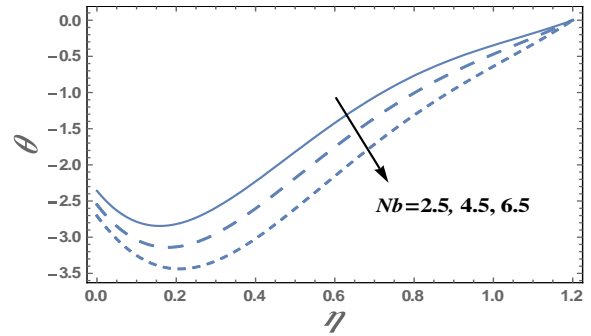


Figure 7: The temperature θ is sketched towards η under the impact of Nb

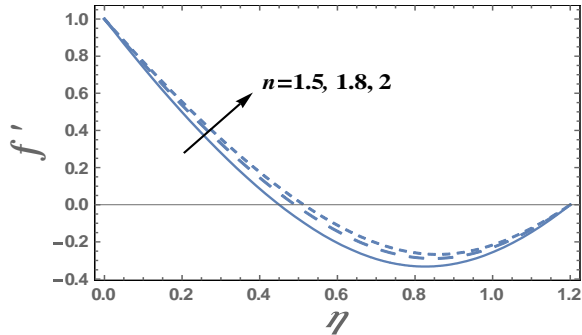


Figure 4: The tangential velocity f' is sketched towards η under the impact of n

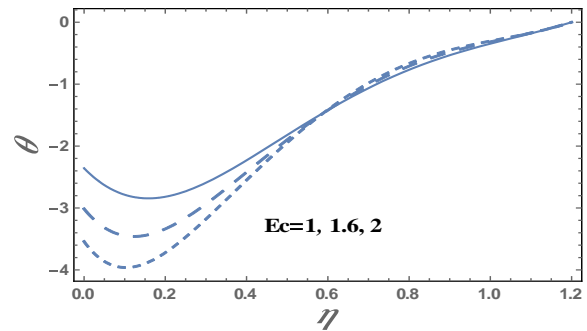


Figure 8: The temperature θ is sketched towards η under the impact of Ec

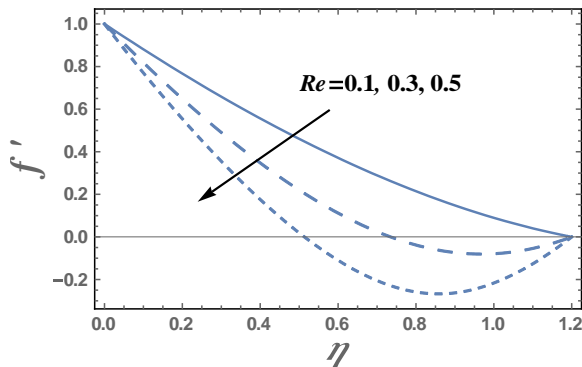


Figure 5: The tangential velocity f' is sketched towards η under the impact of Re

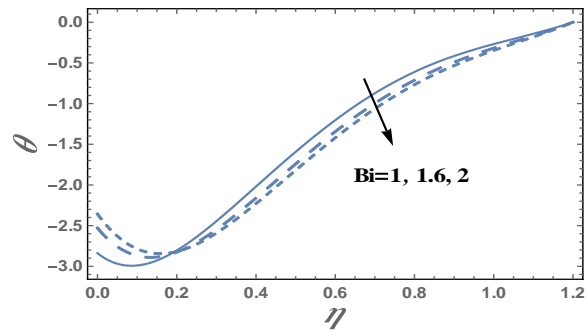


Figure 9: The temperature θ is sketched towards η under the impact of Bi

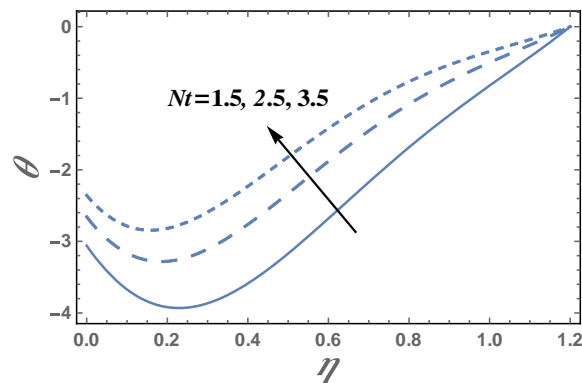


Figure 6: The temperature θ is sketched towards η under the impact of Nt

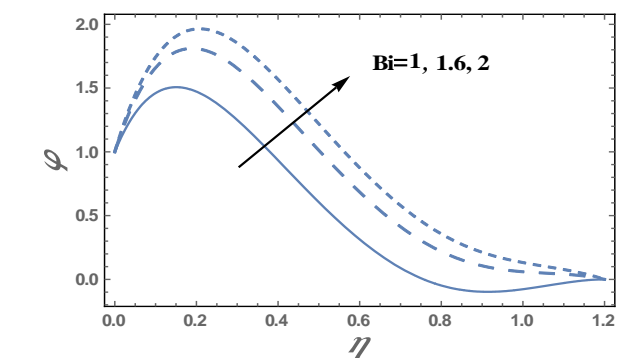


Figure 10: The thenanoparticles concentration φ is sketched towards η under the impact of Bi

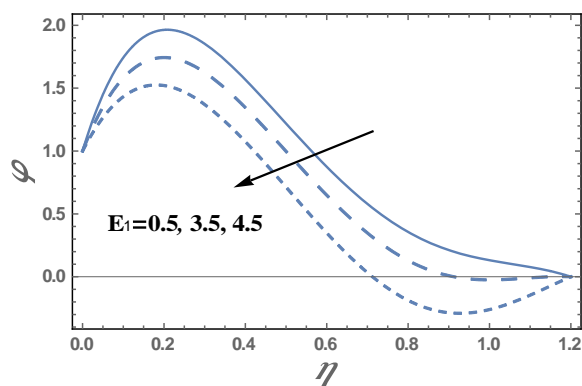


Figure 11: The thenanoparticles concentration ϕ is sketched towards η under the impact of E_1

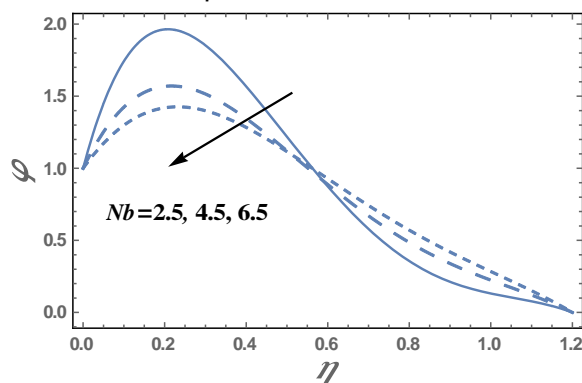


Figure 12: The nanoparticles concentration ϕ is sketched towards η under the impact of Nb

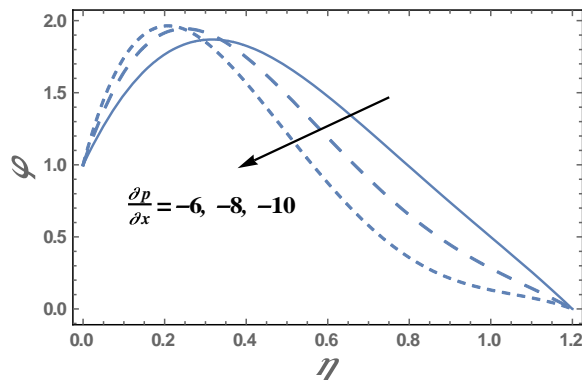


Figure 13: The thenanoparticles concentration ϕ is sketched towards η under the impact of $\frac{\partial p}{\partial x}$

5. Conclusion

This problem is an extension of Eldabe et al. [11] to include both non-Darcian and non-Newtonian nanofluid, viscous dissipation effects. The highly non-linear partial differential equations of velocity, temperature and nanoparticles concentration are converted into non-linear ordinary differential equation by using suitable similarity transformations. This system of equations is solved

numerically by applying Rung-Kutta-Merson-method with a Newton iteration in a shooting and matching technique. The ready analysis can render as a model which may support in comprehension the mechanics of chemical and physiological flows [30-33]. The obtained results can be outlined as follows.

1. By increasing n and We and F_s , both the normal and tangential velocities increase while they decrease as E_1 , M , and Re increase.

2. The normal velocity becomes greater with increasing the dimensionless coordinate η and reaches maximum at $\eta=0.52$, after which, it decreases, but the tangential velocity has an opposite manner, i.e. it has a minimum value.

3. The temperature distribution increases as Da , δ , Nt and Re increase, while it decreases or increases as Bi , Ec , n , Pr , R , Sc and We increase.

4. The temperature becomes lower with increasing the dimensionless coordinate η and reaches minimum at $\eta=0.16$, after which, it increases.

5. The nanoparticles concentration has an opposite behavior with respect to the temperature behavior except that it increases as Bi , n , Sc and We increase.

References

- [1] A. Bejan, A study of entropy generation in fundamental convective heat transfer, ASME J. Heat Transf. 101 (1979) 718-725.
- [2] A. Bejan, Entropy generation minimization: the method of thermodynamic optimization of finite-size systems and finite-time, processes, New York: CRC Press, 51 (1996) 169-180.
- [3] O. M. Haddad, M. K. Alkam, and M. T. Khasawneh, Entropy Generation due to Laminar Forced Convection in the Entrance Region of a Concentric Annulus, Energy, 29 (1)(2004) 35-55.
- [4] L. B. Erbay, M. Ş. Ercan, B. Sülüş, M. M. Yalçın, Entropy Generation During Fluid Flow Between Two Parallel Plates with moving Bottom Plate, Entropy, 5(2003) 506-518.
- [5] A. Z. Sahin, R. Ben-Mansour, Entropy Generation in Laminar Fluid Flow Through a Circular Pipe, Entropy, 5(2003) 404-416.
- [6] B. S. Yilbas, M. Yürüsoy, and M. Pakdemirli, Entropy Analysis for Non-Newtonian Fluid Flow in Annular Pipe: Constant Viscosity Case. Entropy, 6(2004) 304-315.
- [7] H. Alfvén, Existence of electromagnetic-hydrodynamic waves, Nature, 150(1942) 405-406.
- [8] N. Eldabe and M. Abou-Zeid, Radially varying magnetic field effect on peristaltic motion with

- heat and mass transfer of a non-Newtonian fluid between two co-axial tubes, *Therm. Sci.*, 22(2018) 2449-2458
- [9] M. Sheikholeslami, D.D. Ganji, M.Y. Javed and R. Ellahi, Effect of thermal radiation on magnetohydrodynamics nanofluid flow and heat transfer by means of two-phase model, *J. Magn. Main. Mater.*, 374(2015) 36-43.
- [10] M.Y. Abou-zeid, Homotopy perturbation method for couple stresses effect on MHD peristaltic flow of a non-Newtonian nanofluid, *Microsyst. Technol.*, 24(2018) 4839–4846
- [11] N.T. El-Dabe, M.Y. Abou-Zeid, O.H. El-Kalaawy, S.M. Moawad and O.S. Ahmed, Electromagnetic steady motion of Casson fluid with heat and mass transfer through porous medium past a shrinking surface, *Therm. Sci.*, 25(2021) 257-265.
- [12] N. T. M. Eldabe, G. M. Moatimid, M. Abou-zeid, A. A. Elshekhiy and N. F. Abdallah, Semi-analytical treatment of Hall current effect on peristaltic flow of Jeffery nanofluid, *International Journal of Applied Electromagnetics and Mechanics*, 67 (2021), 47-66.
- [13] N. T. Eldabe, M. Y. Abou-zeid, M. A. Mohamed and M. Maged, Peristaltic flow of Herschel Bulkley nanofluid through a non-Darcy porous medium with heat transfer under slip condition, *International Journal of Applied Electromagnetics and Mechanics*, 66 (2021), 649-668.
- [14] N. T. Eldabe and M. Y. Abou-zeid, Magnetohydrodynamic peristaltic flow with heat and mass transfer of micropolar Biviscosity fluid through a porous medium between two co-axial tubes, *Arabian Journal of Science & Engineering*, 39 (2014), 5045–5062.
- [15] N. T. M. Eldabe, M. Y. Abou-zeid, A. Abosaliem, A. Alana, and N. Hegazy, Homotopy perturbation approach for Ohmic dissipation and mixed convection effects on non-Newtonian nanofluid flow between two co-axial tubes with peristalsis, *International Journal of Applied Electromagnetics and Mechanics*, 67 (2021), 153-163.
- [16] N. T. M. Eldabe, M. Y. Abou-zeid, M. E. Ouaf, D. R. Mustafa and Y. M. Mohammed, Cattaneo – Christov heat flux effect on MHD peristaltic transport of Bingham Al_2O_3 nanofluid through a non – Darcy porous medium , *International Journal of Applied Electromagnetics and Mechanics*, 68 (2022), 59-84.
- [17] N. T. M. Eldabe, R. R. Rizkallah, M. Y. Abou-zeid and V. M. Ayad, Thermal diffusion and diffusion thermo effects of Eyring- Powell nanofluid flow with gyrotactic microorganisms through the boundary layer, *Heat Transfer — Asian Res.* 49 (2020), 383 – 405.
- [18] R. Ellahi, S. M. Sait, N. Shehzad, and Z. Ayaz, A hybrid investigation on numerical and analytical solutions of electro-magnetohydrodynamics flow of nanofluid through porous media with entropy generation, *Int. J. Numer. Methods Heat Fluid Flow*, 30(2020), 834-854.
- [19] M. Y. Abou-zeid, Implicit homotopy perturbation method for MHD non-Newtonian nanofluid flow with Cattaneo-Christov heat flux due to parallel rotating disks. *Journal of nanofluids* 8(8) (2019), 1648-1653.
- [20] N. T. Eldabe, G. M. Moatimid, M. Y. Abouzeid, A. A. El-Shekhiy and N. F. Abdallah, Instantaneous thermal-diffusion and diffusion-thermo effects on carreau nanofluid flow over a stretching porous sheet, *J. Adv. Res. Fluid Mech. Therm. Sci.*, 72(2020) 142-157.
- [21] M. Kamran and B. Wiwatanapataphee, Chemical reaction and Newtonian heating effects on steady convection flow of a micropolar fluid with second order slip at the boundary. *Eur. J. Mech. B Fluids*, 71(2018) 138–150.
- [22] M. Y. Abou-zeid, Magnetohydrodynamic boundary layer heat transfer to a stretching sheet including viscous dissipation and internal heat generation in a porous medium, *Journal of porous Media*, 14 (11) (2011), 1007-1018.
- [23] M. El. M. Ouaf and M. Y. Abou-zeid, Electromagnetic and non-Darcy effects on micropolar non-Newtonian fluid boundary-layer flow with heat and mass transfer, *International Journal of Applied Electromagnetics and Mechanics*, 66 (2021), 693-703.
- [24] N. T. M. Eldabe, M. Y. Abou-zeid, S. M. Elshabouri, T. N. Salama and A. M. Ismael, Ohmic and viscous dissipation effects on micropolar non-Newtonian nanofluid Al_2O_3 flow through a non-Darcy porous media, *International Journal of Applied Electromagnetics and Mechanics*, DOI: 10.3233/JAE-210100.
- [25] M. El. M. Ouaf and M. Y. Abou-zeid, Hall currents effect on squeezing flow of non-

- Newtonian nanofluid through a porous medium between two parallel plates, *Case Studies in Thermal Engineering*, 28 (2021), 10362.
- [26] N. T. Eldabe, M. Y. Abou-zeid, A. A. Shaaban and H. A. Sayed, Magnetohydrodynamic non-Newtonian nanofluid flow over a stretching sheet through a non-Darcy porous medium with radiation and chemical reaction, *Journal of Computational and Theoretical Nanoscience*, 12 (2015), 5363-5371.
- [27] M. Y. Abou-zeid, A. A. Shaaban, and M. Y. Alnour, Numerical treatment and global error estimation of natural convective effects on gliding motion of bacteria on a power-law nanoslime through a non-Darcy porous medium, *Journal of Porous Media*, 18 (2015), 1091–1106.
- [28] M. Y. Abou-zeid, and M. A. A. Mohamed, Homotopy perturbation method for creeping flow of non-Newtonian Power-Law nanofluid in a nonuniform inclined channel with peristalsis. *Z. Naturforsch* 72 ((10)a) (2017), 899–907.
- [29] M. A. Mohamed, and M. Y. Abou-Zeid, MHD peristaltic flow of micropolar Casson nanofluid through a porous medium between two co-axial tubes. *J Porous Media* .22 (9) (2019), 1079-1093.
- [30] W. Abbas, Nabil T. M. Eldabe, Rasha A. Abdelkhalek, Nehad, A. Zidan and S. Y. Marzouk, Soret and Dufour Effects with Hall Currents on Peristaltic Flow of Casson Fluid with Heat and Mass Transfer Through Non-Darcy Porous Medium Inside Vertical Channel, *Egyptian Journal of Chemistry* **64** (2021), 5217-5227.
- [31] M. A. Batiha, M. M. Dardir, H. Abuseda, N. A. Negm and H. E. Ahmed, Improving the performance of water-based drilling fluid using amino acid-modified graphene oxide nanocomposite as a promising additive, *Egyptian Journal of Chemistry* **64** (2021), 1799-1806.
- [32] M. Ibrahim, N. Abdallah and M. Abouzeid, Activation energy and chemical reaction effects on MHD Bingham nanofluid flow through a non-Darcy porous media, *Egyptian Journal of Chemistry* Doi: 10.21608/EJCHEM.2022.117814.5310.
- [33] A. Ismael, N. Eldabe, M. Abouzeid and S. Elshabouri, Activation energy and chemical reaction effects on MHD Bingham nanofluid flow through a non-Darcy porous media, *International Journal of Applied Electromagnetics and Mechanics*, Doi: 10.21608/EJCHEM.2022.120066.5388.
- [34] M. E. Ouaf, M. Y. Abouzeid and Y. M. Younis, Entropy generation and chemical reaction effects on MHD non-Newtonian nanofluid flow in a sinusoidal channel Doi: 10.3233/JAE-210215.
- [35] N. T. Eldabe, S. Elshabouri, H. Elarabawy, M. Y. Abouzeid and A. Abuiyada, Wall properties and Joule heating effects on MHD peristaltic transport of Bingham non-Newtonian nanofluid , *International Journal of Applied Electromagnetics and Mechanics*, Doi: 10.3233/JAE-210126,
- [36] N. T. M. Eldabe, R. R. Rizkallah, M. Y. Abou-zeid and V. M. Ayad, Effect of induced magnetic field on non-Newtonian nanofluid Al₂O₃ motion through boundary-layer with gyrotactic microorganisms, *Thermal Science*, 26 (2022), 411 – 422.
- [37] N. T. M. Eldabe, M. Y. Abou-zeid, M. A. A. Mohamed and M. M. Abd-Elmoneim, MHD peristaltic flow of non-Newtonian power-law nanofluid through a non-Darcy porous medium inside a non-uniform inclined channel, *Archive of Applied Mechanics* 91 (2021), 1067–1077.
- [38] M. Y. Abou-zeid, Homotopy perturbation method to gliding motion of bacteria on a layer of power-law nanoslime with heat transfer, *J. Comput. Theor. Nanosci.* 12 (2015) 3605–3614.
- [39] N. T. M. Eldabe, M. Y. Abouzeid, and H.A. Ali, Effect of heat and mass transfer on Casson fluid flow between two co-axial tubes with peristalsis, *J. Adv. Res. Fluid Mech. Therm. Sci.* 76(1) 2020 54-75.
- [40] H. M. Mansour and M. Y. Abouzeid, Heat and mass transfer effect on non-newtonian fluid flow in a non-uniform vertical tube with peristalsis, *J. Adv. Res. Fluid Mech. Therm. Sci.* 61 (1) (2019) 44-64.